Effects of electron correlation on thermodynamic properties of expanded alkali fluids

Effects of electron correlation on thermodynamic properties of expanded alkali fluids

I Ishida[1]

Hiroshima Institute of Technology, 2-1-1 Miyake, Saiki Ward, Hiroshima 731-5193, Japan

E-mail: ikuji@do2.enjoy.ne.jp

Abstract
On the basis of the lattice-gas Hubbard model, which is the extension of the original Hubbard model for a crystal to the lattice-gas system, the thermodynamic properties of expanded alkali fluids are investigated to clarify how electron correlation, which causes the metal–non-metal transition in these fluids, influences their thermodynamic behaviours near the critical point of the liquid–vapour (LV) transition, and especially at the transition itself. The thermodynamic potential is calculated in a self-consistent combination of approximations: the molecular-field approximation for treating random atomic arrangements and the single-site coherent-potential approximation due to Yonezawa and Watabe for dealing with electron correlation. The results calculated for the equation of state are analysed in detail and it is pointed out that the peculiar behaviour of the LV transition observed for fluid caesium could be caused by the effects of electron correlation.

1. Introduction

Expanded fluids of metallic elements in the vicinity of the critical point of the liquid–vapour (LV) transition have been attracting much attention for quite a long time. References to most of the important work in the research on these systems can be found, for example, in [1]—in particular in a review paper by Yonezawa and Ogawa [2] in [1].

The main interest in the investigation of these systems is in how the metal–non-metal (MNM) transition, which should occur in these systems somewhere around the critical point, is related to the LV transition. There are three main possible mechanisms for the MNM transition: narrowing and subsequent splitting of electron energy bands with decreasing density (the Wilson transition); localization of electrons due to electron correlation (the Mott transition); and localization induced by disorder in the microscopic atomic arrangement (the Anderson or percolation transition). In actual fluid metals some combinations of these mechanisms act

[1] Permanent address: 1-25-29 Sendou, Saiki-Ward, Hiroshima 731-5141, Japan.

to cause the MNM transition. For alkali metals, which are monovalent, the Mott transition combined with the effect of disorder is considered to occur. For polyvalent metals such as mercury, the MNM transition is usually accounted for as being caused by a combination of the Wilson and the Anderson mechanism.

In this paper, we are concerned with the role of the electron correlation in determining the thermodynamic properties, especially the LV transition of alkali metals. The following important experimental facts are relevant to the present investigation. The density dependence of the electrical conductivity already departs from the nearly-free-electron behaviour at relatively high densities, i.e. $\rho \lesssim 2\rho_c$ where ρ_c is the critical density [3]. The static susceptibility data [4] also suggest that the electron correlation becomes essential at high densities well above ρ_c. Experiments on the structure factor [5, 6] show that, with decreasing density from the triple point toward the critical region along the vapour pressure line, the coordination number, i.e. the number of nearest-neighbour ions, decreases but the nearest-neighbour distance remains almost constant.

Taking these facts into consideration, a model, which we shall call the lattice-gas Hubbard model, has been investigated rather extensively (see, for a review, [2]). The model is the extension of the original Hubbard model for a crystalline system to a lattice-gas system and is described by the following Hamiltonian:

$$\hat{H} = \hat{H}_a + \hat{H}_e \tag{1}$$

$$\hat{H}_a = -\tfrac{1}{2} \sum_{i \neq j} J_{ij} \xi_i \xi_j \tag{2}$$

$$\hat{H}_e = E_0 \sum_{i,\sigma} n_{i\sigma} \xi_i + \sum_{i \neq j,\sigma} V_{ij} a_{i\sigma}^{\dagger} a_{j\sigma} \xi_i \xi_j + \frac{U}{2} \sum_{i,\sigma} n_{i\sigma} n_{i-\sigma} \xi_i \tag{3}$$

where the random variable ξ_i at the ith site takes a value 1 or 0 according to whether an ion occupies the site or not, and therefore $\sum_i \xi_i = \hat{N}_a$, $\hat{N}_a$ being the total number of ions in the system. The total volume of the system, the total number of sites, and the unit-cell volume of the underlying regular lattice are denoted by V, N, and v_0 respectively; by definition they are related as $V = N v_0$. $\hat{H}_a$ is the Hamiltonian for the atomic system, $\hat{H}_e$ the Hamiltonian for the electronic system, $a_{i\sigma}$ ($a_{i\sigma}^{\dagger}$, $n_{i\sigma} = a_{i\sigma}^{\dagger} a_{i\sigma}$) the annihilation (creation, number) operator of an electron with spin σ at the ith site. E_0 is an atomic energy of the s orbital, V_{ij} the hopping integral for hopping between ions at the ith and the jth site and, U the intra-atomic Coulomb interaction between electrons. The interaction J_{ij} between the ith and the jth ion is supposed to describe the direct inter-ionic Coulomb interaction as well as the indirect effects due to the ion–electron and the electron–electron interactions at different sites and possibly the Van der Waals interactions. The double summations over sites i and j in equations (2) and (3) are taken over all nearest-neighbour sites (see [2] for more detail).

The electronic properties of expanded alkali fluids were first investigated on the basis of the lattice-gas Hubbard model by Yonezawa and Watabe [7]. They proposed a single-site coherent-potential formalism which is the extension of the alloy-analogy approximation for the original Hubbard model for crystals to the case of the lattice gas, and discussed the effect of disorder on the Mott–Hubbard transition. The thermodynamic properties of the lattice-gas Hubbard system were first studied rather extensively by Nara *et al* [8] on the basis of a combination of the Takagi method and the Gutzwiller variation method for treating the statistical averaging of the atomic arrangement and the electron correlation respectively. They analysed the phase diagrams for this system with a wide range of the model parameters contained in the Hamiltonian (1) and showed that quite a variety of types of phase diagram could be obtained. A similar investigation was performed by us (unpublished work referred

to in [1]) by employing the mean-field approximation for averaging over atomic arrangements and, to be consistent with the mean-field approximation, the coherent-potential method given by Yonezawa and Watabe [7] for the electron correlation. It was shown that the different treatments of the electron correlation as well as the atomic arrangements lead to quite different results for phase diagrams. These investigations were reviewed and extended somewhat by Yonezawa and Ogawa [2]; in particular, they presented a simple method for calculating the ground-state energy of the electron system including the electron-correlation effect in the coherent-potential approximation, which had been obtained either numerically or by a more tedious method in the previous work.

After these theoretical studies, around 1980 much detailed experimental work on the thermodynamic properties of expanded Rb and Cs fluids was done by Hensel and co-workers [9, 10]. They demonstrated that, in contrast to the case for simple fluids such as fluid Ar, the LV coexistence curve, i.e. the curve describing the boundary of the coexisting liquid and vapour phases on the volume versus temperature plane, is strongly asymmetric and the law of the rectilinear diameter breaks down over a large temperature range for fluid alkalis such as Rb and Cs. Among recent theoretical research in relation to the above experimental results, the work most relevant to the present paper is that by Reinaldo-Falagán *et al* [11, 12]. In the earlier paper [11], using a model which is the single-particle version of the lattice-gas Hubbard model presented above, and a self-consistent method for determining the ionic configurations and the electronic energies, they obtained results for the thermodynamic and electronic properties of expanded alkali fluids which agree qualitatively with the experimental results. In particular, they concluded that the extreme asymmetry of the coexistence curves is reproduced by taking account self-consistently of the effect of the local coordination in determining the free energy per ion. Most recently [12], they modified their previous work to include the effects of electron correlation. Their theory is an extension of the work by Nara *et al*; they employed the Gutzwiller approximation for the lattice-gas Hubbard model at finite temperatures and determined the electronic and atomic distributions self-consistently as in their previous work. Their numerical results show that the thermodynamic properties and the electric conductivity are not essentially affected by electron correlation, and the MNM transition in their theory is of the classical percolation type rather than the Mott type.

The purpose of this paper is to revisit the lattice-gas Hubbard model in the light of the recent experimental and theoretical progress and to show that our results, which were obtained using our old theory, can reproduce the peculiar behaviour of the coexistence curve of fluid alkalis in the critical region with a proper choice of the model parameters. For convenience of reference, our formulation is presented in some detail in section 2. In section 3, the relationship between the MNM and the LV transition is discussed and it is pointed out that a variety of phase diagrams can be obtained by varying the strength of the electron correlation. Following these general analyses, the peculiar behaviour of the coexistence curve of fluid Cs is discussed in the same section. The final section is devoted to our conclusions.

2. Formulation

In this section the formulation employed in this paper is presented. The thermodynamic potential of the lattice-gas Hubbard model is calculated by adopting the mean-field approximation for random averaging over atomic configurations and then, to be consistent with the mean-field approximation, the coherent-potential approximation for calculating the electronic contribution to the thermodynamic potential. We also present the analytic expressions for the thermodynamic potential and the equation of state which can be obtained by assuming a simple form for the electronic density of states for the underlying regular lattice. We shall use these expressions to analyse the experimental results for fluid Cs in the following section.

2.1. Thermodynamic potential

The thermodynamic potential Ω of the lattice-gas Hubbard system can be calculated in the following two steps: the quantum-mechanical trace $\mathrm{Tr}^{(e)}$ over electron states is first performed for a fixed ion configuration $\{\xi_i\}$ and then the trace $\mathrm{Tr}^{(a)}$ over the ionic configurations is taken. Thus we obtain

$$
\begin{aligned}
\Omega = -PV &= -\beta^{-1} \ln \mathrm{Tr}^{(a)} \, \mathrm{Tr}^{(e)} \exp\{-\beta(\hat{H} - \mu_e \hat{N}_e - \mu_a \hat{N}_a)\} \\
&= -\beta^{-1} \ln \mathrm{Tr}^{(a)} \exp\{-\beta(\hat{H}_{\mathrm{eff}}[\{\xi_i\}] - \mu_a \hat{N}_a)\}
\end{aligned}
\tag{4}
$$

in terms of the effective Hamiltonian defined as

$$
\hat{H}_{\mathrm{eff}}[\{\xi_i\}] = \hat{H}_a + \hat{\Omega}_e[\{\xi_i\}] \tag{5}
$$

$$
\hat{\Omega}_e[\{\xi_i\}] = -\beta^{-1} \ln \mathrm{Tr}^{(e)} \exp\{-\beta(\hat{H}_e - \mu_e \hat{N}_e)\}. \tag{6}
$$

Here, P is the pressure, $\beta = (k_B T)^{-1}$ with k_B the Boltzmann constant and T the temperature, $\hat{N}_e = \sum_{i,\sigma} n_{i\sigma} \xi_i$ is the total number operator for the electrons, and μ_a and μ_e are the chemical potentials for the atomic and the electronic system, respectively.

The average total numbers of atoms and electrons are obtained in the standard way as

$$
N_a = -\frac{\partial \Omega}{\partial \mu_a} \tag{7}
$$

$$
N_e = -\frac{\partial \Omega}{\partial \mu_e}. \tag{8}
$$

The chemical potentials μ_a and μ_e are determined by solving equations (7) and (8).

The condition for charge neutrality in this system relates these numbers to each other as follows:

$$
N_a = N_e = N\xi \tag{9}
$$

where ξ is the average value of ξ_i. The atomic volume v_a, which is the volume per atom, is expressed in terms of ξ as

$$
v_a = V/N_a = v_0/\xi. \tag{10}
$$

The conditions for thermal equilibrium between two phases (1) and (2) with volume $V^{(1)}$ and $V^{(2)}$ respectively at temperature T are given as usual by

$$
\begin{aligned}
P &= P^{(1)}(V^{(1)}) = P^{(2)}(V^{(2)}) \\
\mu_e^{(1)}(P, T) &= \mu_e^{(2)}(P, T) \\
\mu_a^{(1)}(P, T) &= \mu_a^{(2)}(P, T).
\end{aligned}
\tag{11}
$$

2.2. Thermodynamic potential in the mean-field approximation

The electronic thermodynamic potential $\hat{\Omega}_e[\{\xi_i\}]$ involved in the effective Hamiltonian (5) can be expressed in general as the sum over many-body interaction terms by the cumulant expansion method [14]:

$$
\hat{\Omega}_e[\{\xi_i\}] = \sum_{n=1}^{\infty} \frac{1}{n!} \sum_{i_1, i_2, \ldots, i_n}{}' \omega_n(i_1, i_2, \ldots, i_n) \xi_{i_1} \xi_{i_2} \cdots \xi_{i_n}. \tag{12}
$$

where the sum over $i_1, i_2, \ldots, i_n$ is taken over different sites. Introducing an effective field acting on the ion on ith site defined by

$$
\hat{\phi}_{\mathrm{eff}}(i) = \sum_{i_2, \ldots, i_{n-1}}{}' \omega_n(i, i_2, \ldots, i_{n-1}) \xi_{i_2} \xi_{i_3} \cdots \xi_{i_{n-1}} \tag{13}
$$

we can rewrite (6) as

$$\hat{\Omega}_{\mathrm{e}}[\{\xi_i\}] = \sum_i \hat{\phi}_{\mathrm{eff}}(i)\xi_i. \tag{14}$$

It is noted that the relationship between the asymmetry of the coexistence curve and the presence of many-body (or state-dependent) effective interactions among ions was discussed by Goldstein *et al* (see [13] and references therein). However, as discussed below, a different cause of the asymmetric coexistence curve is proposed in this paper.

Using the mean-field approximation that the ion on each site in the system feels the same average field, that is, $\phi_{\mathrm{eff}}^{\mathrm{mfa}} = \langle \hat{\phi}_{\mathrm{eff}}(i) \rangle^{\mathrm{mfa}}$, we calculate the grand partition function and the thermodynamic potential using the following set of equations:

$$\Xi^{\mathrm{mfa}} = \exp(-\beta \Omega^{\mathrm{mfa}}) = \mathrm{Tr}^{(\mathrm{a})} \exp\{-\beta(\hat{H}_{\mathrm{eff}}^{\mathrm{mfa}}[\{\xi_i\}] - \mu_{\mathrm{a}} \hat{N}_{\mathrm{a}})\} \tag{15}$$

$$\Omega^{\mathrm{mfa}} = \Omega_{\mathrm{a}}^{\mathrm{mfa}} + \Omega_{\mathrm{e}}^{\mathrm{mfa}} \tag{16}$$

$$\frac{\Omega_{\mathrm{a}}^{\mathrm{mfa}}}{N_{\mathrm{a}}} = -\frac{1}{2}zJ\xi + \beta^{-1}\left\{\ln\xi + \frac{1-\xi}{\xi}\ln(1-\xi)\right\} - \mu_{\mathrm{a}} \tag{17}$$

$$\Omega_{\mathrm{e}}^{\mathrm{mfa}} = \langle \hat{\Omega}_{\mathrm{e}}[\{\xi_i\}] \rangle^{\mathrm{mfa}} \tag{18}$$

$$\hat{H}_{\mathrm{eff}}^{\mathrm{mfa}}[\{\xi_i\}] = \phi_{\mathrm{eff}}^{\mathrm{mfa}} \sum_i \xi_i + \frac{1}{2}NzJ\xi^2 - \xi^2 \frac{\partial}{\partial \xi}\left(\frac{\Omega_{\mathrm{e}}^{\mathrm{mfa}}}{\xi}\right) \tag{19}$$

$$\phi_{\mathrm{eff}}^{\mathrm{mfa}} = \left\langle \frac{\partial \hat{H}_{\mathrm{eff}}^{\mathrm{mfa}}[\{\xi_i\}]}{\partial \xi_i} \right\rangle^{\mathrm{mfa}} = -zJ\xi + \frac{1}{N}\frac{\partial \Omega_{\mathrm{e}}^{\mathrm{mfa}}}{\partial \xi} \tag{20}$$

$$\xi = \langle \xi_i \rangle^{\mathrm{mfa}} = [\exp\{\beta(\phi_{\mathrm{eff}}^{\mathrm{mfa}} - \mu_{\mathrm{a}})\} + 1]^{-1} \tag{21}$$

$$\langle(\cdots)\rangle^{\mathrm{mfa}} = \frac{1}{\Xi^{\mathrm{mfa}}} \mathrm{Tr}^{(\mathrm{a})}(\cdots)\exp\{-\beta(\hat{H}_{\mathrm{eff}}^{\mathrm{mfa}}[\{\xi_i\}] - \mu_{\mathrm{a}}\hat{N}_{\mathrm{a}})\} \tag{22}$$

where $\langle(\cdots)\rangle^{\mathrm{mfa}}$ is the statistical average of the physical quantity $(\cdots)$ for the atomic system. z is the number of nearest-neighbour sites. The relation $\langle \hat{H}_{\mathrm{eff}}[\{\xi_i\}] \rangle^{\mathrm{mfa}} = \langle \hat{H}_{\mathrm{eff}}^{\mathrm{mfa}}[\{\xi_i\}] \rangle^{\mathrm{mfa}}$ is automatically satisfied. Hereafter, we eliminate the notation 'mfa' for brevity. Note that the thermodynamic potential (16) satisfies the minimum condition:

$$\frac{1}{N}\frac{\partial \Omega}{\partial \xi} = \phi_{\mathrm{eff}} + \beta^{-1}\{\ln\xi - \ln(1-\xi)\} - \mu_{\mathrm{a}} = 0 \tag{23}$$

which is nothing but equation (21). From $\Omega = -PV$, the equation of state is obtained as

$$Pv_0 = -\frac{1}{2}zJ\xi^2 - \beta^{-1}\ln(1-\xi) + \frac{\xi^2}{N}\frac{\partial}{\partial \xi}\left(\frac{\Omega_{\mathrm{e}}}{\xi}\right). \tag{24}$$

The above equation without the electronic contributions is the well-known result for the pressure in the lattice-gas model.

2.3. Electronic thermodynamic potential in the coherent-potential approximation

In order to calculate the thermodynamic potential (18), we need to introduce some approximations. Firstly, we assume the effect of temperature for the electronic system to be small and replace Ω_{e} by the value at zero temperature, i.e. $E_{\mathrm{e}}^{(0)} - \mu_{\mathrm{e}}N_{\mathrm{e}}$ where $E_{\mathrm{e}}^{(0)}$ is the ground-state energy. As is well known, it is convenient to employ the Green function method, in which $E_{\mathrm{e}}^{(0)}$ and N_{e} are expressed in terms of the Green function $G^{\sigma}(k, E)$ as follows:

$$E_{\mathrm{e}}^{(0)} = -\frac{1}{\pi\hbar}\sum_{k,\sigma}\mathrm{Im}\int_{-\infty}^{\mu_{\mathrm{e}}}\mathrm{d}x\left\{x - \frac{1}{2}\Sigma^{\sigma}(k, x)\right\}G^{\sigma}(k, x) \tag{25}$$

$$N_{\mathrm{e}} = -\frac{1}{\pi\hbar} \sum_{k,\sigma} \mathrm{Im} \int_{-\infty}^{\mu_{\mathrm{e}}} \mathrm{d}x \, G^{\sigma}(k, x) \tag{26}$$

where the self-energy $\Sigma^{\sigma}(k, E)$ is defined by

$$G^{\sigma}(k, E) = \lim_{\delta \to +0} \frac{\hbar}{E + \mathrm{i}\delta - E(k) - \Sigma^{\sigma}(k, E)} \tag{27}$$

with the band energy for the underlying regular lattice given by

$$E(k) = E_0 + \sum_{j(\neq i)} V_{ij} \exp\{\mathrm{i}k \cdot (R_j - R_i)\}.$$

The derivation of this expression is given in the appendix.

Then, in order to calculate the Green function, a further approximation is needed. To be consistent with the mean-field approximation for atomic configurations, we adopt the single-site coherent-potential method due to Yonezawa and Watabe [7], which is the extension to the lattice-gas system of the alloy-analogy approximation of the Hubbard model for crystals. In this method, the self-energy is assumed to be site diagonal (i.e. independent of k) and the Green function is determined by solving self-consistently the following set of equations and (27):

$$F^{\sigma}(E) = \frac{\xi(1 - n_{-\sigma})F^{\sigma}(E)}{1 + \hbar^{-1}\Sigma^{\sigma}(E)F^{\sigma}(E)} + \frac{\xi n_{-\sigma} F^{\sigma}(E)}{1 - \hbar^{-1}(U - \Sigma^{\sigma}(E))F^{\sigma}(E)} \tag{28}$$

$$F^{\sigma}(E) = \frac{1}{N} \sum_{k} G^{\sigma}(k, E) = \int_{-\infty}^{\infty} \mathrm{d}x \, \frac{\hbar D_0(x)}{E + \mathrm{i}\delta - x - \Sigma^{\sigma}(E)} \tag{29}$$

where $D_0(x)$ is the density of electronic states of the underlying periodic lattice defined by

$$D_0(E) = \frac{1}{N} \sum_{k} \delta(E - E(k)). \tag{30}$$

The function $F^{\sigma}(E)$ is the averaged site-diagonal Green function, in terms of which the averaged density of states per atom for electrons with spin σ, $D^{\sigma}(E)$, is given by

$$D^{\sigma}(E) = -\frac{1}{\pi\hbar\xi} \mathrm{Im} \, F^{\sigma}(E). \tag{31}$$

The quantity n_{σ} in (28) is the averaged number per atom of electrons with spin σ and can be written in terms of $D^{\sigma}(E)$ as

$$n_{\sigma} = \int_{-\infty}^{\mu_{\mathrm{e}}} \mathrm{d}x \, D^{\sigma}(x). \tag{32}$$

Note that the condition $n_{\uparrow} + n_{\downarrow} = 1$ determines the electronic chemical potential (Fermi energy) μ_{e}.

When the parameter ξ is decreased with a fixed U, we obtain the transition (Mott transition) from a metallic state, for which the density of states $D^{\sigma}(E)$ is finite and continuous at the Fermi energy μ_{e}, to a non-metallic state, for which the single band in the metallic state splits into two at μ_{e}.

For the non-magnetic system considered here, where $n_{\uparrow} = n_{\downarrow}$, the Green function $G^{\sigma}(k, E)$ and the self-energy $\Sigma^{\sigma}(E)$ are independent of σ. Dropping the suffix σ for simplicity, we can calculate the electronic thermodynamic potential per atom as

$$\frac{\Omega_{\mathrm{e}}}{N_{\mathrm{e}}} = -\frac{2}{\pi\hbar\xi} \mathrm{Im} \int_{-\infty}^{\mu_{\mathrm{e}}} \mathrm{d}x \, F(x) \left(x - \frac{1}{2}\Sigma(x) - \mu_{\mathrm{e}} \right). \tag{33}$$

The factor 2 is due to the degeneracy of spins.

It is possible to calculate numerically all physical quantities from the total thermodynamic potential (16) which is composed of (17) and (33).
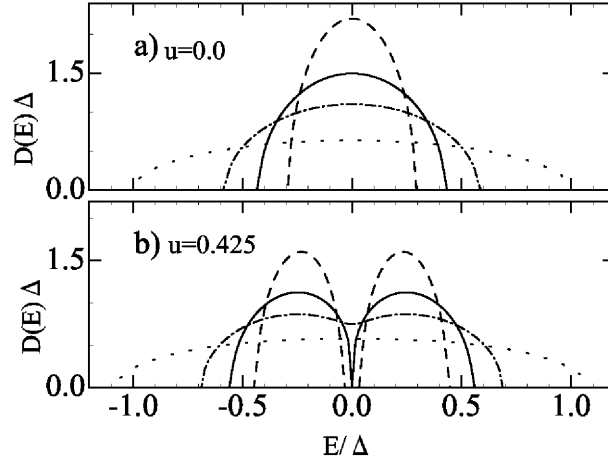
Figure 1. Calculated densities of states for (a) $u = 0.0$ and (b) $u = 0.425$ at: $v = 1.0$ (- - - -); $v = 4.0$ (— · —); $v = 5.536$ (——); and $v = 11.1$ (— — —). The energy is scaled by the half-bandwidth Δ of the regular lattice and its origin is chosen to be the chemical potential value.

3. Application

3.1. Analytic expression of the thermodynamic potential with a simple density of states for the regular lattice

In order to understand the essential features of the electronic contributions to the thermodynamic properties of alkali fluids near their critical points on the basis of the formulation described in the previous section, it is convenient to have analytic expressions for thermodynamic quantities. This can be achieved by assuming the density of states for the underlying regular lattice to take a simple elliptic form:

$$D_0(E) = \frac{2}{\pi \Delta^2} \sqrt{\Delta^2 - (E - E_0)^2} \tag{34}$$

with Δ the half-bandwidth. Then, for the non-magnetic system, where $n_\uparrow = n_\downarrow = 1/2$, the density of states $D(E)$ becomes symmetric with respect to $\mu_e = E_0 + U/2$ and we can obtain Ω_e in an analytic form [2]. We use Δ as a scaling parameter for energies. Then, the scaled electronic thermodynamic potential per atom, $\omega_e \equiv \Omega_e/(N_e \Delta)$, is described by just two parameters, $u = U/\Delta$ and the reduced atomic volume $v = v_a/v_0 = 1/\xi$.

When the parameter v is increased, that is, the atomic density ρ is decreased, the Mott transition takes place at the reduced volume $v_M = 1/u^2$ as determined by the condition of $D(\mu_e) = 0$. The typical results with $u = 0.425$ are shown for various values of $v = 1.0, 4.0$, 5.536, and 11.1 in figure 1(b). For comparison the results with $u = 0$ are also shown. On increasing v, the density of states with $u = 0$, which is, at $v = 1.0$, identical to the one for the regular lattice (shown by the dashed line in figure 1(a)), gets narrower but remains a single band. On the other hand, for $u = 0.425$, the density of states, which is already different from the one for the regular lattice at $v = 1.0$ due to the effect of finite u, remains a single band for $v \lesssim v_M = 5.536$, but for $v \gtrsim v_M = 5.536$ it becomes split into two bands.

For the purpose of investigating how the LV transition is affected by the electron-correlation effect, we divide ω_e into two parts: a part for a system of free electrons with $u = 0$, $\omega_e^{(0)}$; and a part describing the effect of electron correlation, $\omega_e^{(1)}$:

$$\omega_e = \omega_e^{(0)} + \omega_e^{(1)} \tag{35}$$

$$\omega_{\mathrm{e}}^{(0)} = -\frac{4}{3\pi\sqrt{v}} \tag{36}$$

$$\omega_{\mathrm{e}}^{(1)} = -\frac{3\sqrt{v_{\mathrm{M}}}}{16v} - \frac{1}{2\sqrt{v_{\mathrm{M}}}} + \frac{4}{3\pi\sqrt{v}} + \theta(v_{\mathrm{M}} - v)\frac{1}{24\pi\sqrt{v_{\mathrm{M}}}}$$

$$\times \left\{ 3\left(\frac{3v_{\mathrm{M}}}{v} + 4\right)\arccos\sqrt{\frac{v}{v_{\mathrm{M}}}} - \left(23 - \frac{2v}{v_{\mathrm{M}}}\right)\sqrt{\frac{v_{\mathrm{M}}}{v} - 1}\right\}. \tag{37}$$

By substituting the above results into (24) we obtain the pressure in reduced units as

$$\frac{Pv_0}{\Delta} \equiv p = -\frac{j}{2v^2} + p_{\mathrm{e}}^{(0)} + p_{\mathrm{e}}^{(1)} - t\ln\left(1 - \frac{1}{v}\right) \tag{38}$$

$$p_{\mathrm{e}}^{(0)} = -\frac{2}{3\pi\sqrt{v^3}} \tag{39}$$

$$p_{\mathrm{e}}^{(1)} = -\frac{3\sqrt{v_{\mathrm{M}}}}{16v^2} + \frac{2}{3\pi\sqrt{v^3}}$$

$$+ \theta(v_{\mathrm{M}} - v)\frac{1}{24\pi\sqrt{v_{\mathrm{M}}}}\left\{\frac{9v_{\mathrm{M}}}{v^2}\arccos\sqrt{\frac{v}{v_{\mathrm{M}}}} - \left(\frac{2}{v_{\mathrm{M}}} + \frac{7}{v}\right)\sqrt{\frac{v_{\mathrm{M}}}{v} - 1}\right\} \tag{40}$$

where $j = zJ/\Delta$ and $t = k_{\mathrm{B}}T/\Delta$ is the reduced temperature. $p_{\mathrm{e}}^{(0)}$ and $p_{\mathrm{e}}^{(1)}$ are the contributions to pressure due to $\omega_{\mathrm{e}}^{(0)}$ and $\omega_{\mathrm{e}}^{(1)}$ respectively.

Correspondingly the atomic chemical potential is obtained from (20) and (23) as

$$\mu_{\mathrm{a}}/\Delta = -t\ln(v - 1) + \omega_{\mathrm{e}} + vp_{\mathrm{e}} = -t\ln(v - 1) - \frac{1}{2\sqrt{v_{\mathrm{M}}}} - \frac{3\sqrt{v_{\mathrm{M}}}}{8v}$$

$$+ \theta(v_{\mathrm{M}} - v)\frac{1}{4\pi\sqrt{v_{\mathrm{M}}}}\left\{\left(\frac{3v_{\mathrm{M}}}{v} + 2\right)\arccos\sqrt{\frac{v}{v_{\mathrm{M}}}} - 5\sqrt{\frac{v_{\mathrm{M}}}{v} - 1}\right\}. \tag{41}$$

The dependence of $\omega_{\mathrm{e}}^{(0)}$ on the reduced volume v is due to the ordinary effects of hopping of free electrons; the bandwidth for the free-electron system is proportional to $\sqrt{\xi}$ or to $1/\sqrt{v}$. The dependence of $\omega_{\mathrm{e}}^{(1)}$ on v differs according to whether the electronic system is in the metallic state ($v \leqslant v_{\mathrm{M}}$) or not ($v > v_{\mathrm{M}}$). However, as the lowest-order term in the expansion of $\omega_{\mathrm{e}}^{(1)}$ with respect to $|1 - v/v_{\mathrm{M}}| \ll 1$ in the vicinity of the Mott transition is given by

$$\omega_{\mathrm{e}}^{(1)} + \frac{3\sqrt{v_{\mathrm{M}}}}{16v} + \frac{1}{2\sqrt{v_{\mathrm{M}}}} - \frac{4}{3\pi\sqrt{v}} \simeq \theta(v_{\mathrm{M}} - v)\frac{2}{15\pi\sqrt{v_{\mathrm{M}}}}\left(1 - \frac{v}{v_{\mathrm{M}}}\right)^{5/2} \tag{42}$$

the pressure becomes a smooth and continuous function with respect to v. Note that, for $v > v_{\mathrm{M}}$, ω_{e} is simply given by $-1/(2\sqrt{v_{\mathrm{M}}}) - 3\sqrt{v_{\mathrm{M}}}/(16v)$. The v-dependent second term describes the effects of hopping in this case; the width of each split Hubbard band is due to the process in which an electron with up (or down) spin hops to a nearest-neighbour site occupied by an electron with the opposite spin and then returns to the original site, so it is proportional to ξ or to v^{-1}.

In the analysis presented in the following subsection of possible phase diagrams with varying strength of the electron correlation u, the dependence of $p_{\mathrm{e}}^{(1)}$ on volume v plays an important role. $p_{\mathrm{e}}^{(1)}$ is a positive quantity and increases gradually as v increases but it continues to take small values on the metallic side of the Mott transition, that is for $v < v_{\mathrm{M}}$. In the region of $v \simeq v_{\mathrm{M}}$ it increases abruptly and takes a maximum value $p_{\mathrm{e}}^{(1)} = (4/3\pi)^4 v_{\mathrm{M}}^{-1.5}$ at $v = (3\pi/8)^2 v_{\mathrm{M}} \simeq 1.39 v_{\mathrm{M}}$ on the non-metallic side of the Mott transition. It is noted that the above behaviour of $p_{\mathrm{e}}^{(1)}$ arises from the different v-dependences of the hopping effects for $v \leqslant v_{\mathrm{M}}$ and $v > v_{\mathrm{M}}$ mentioned above.
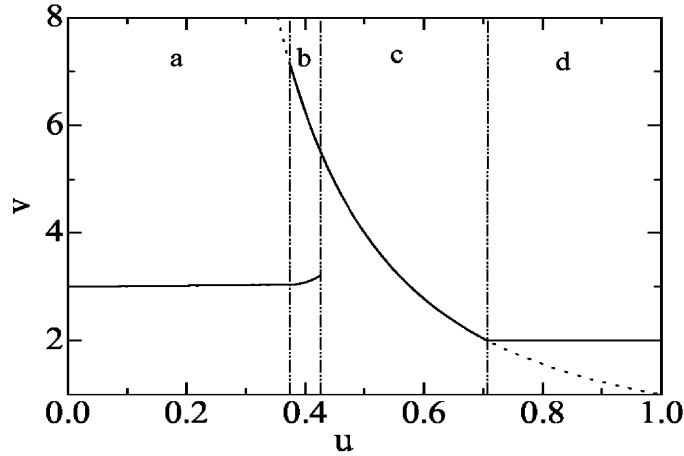
Figure 2. The phase diagram in the (u, v) plane. The solid curve describes the calculated critical atomic volume v_c at which the first-order phase transition is obtained. The Mott transition occurs at the volume v_M shown by the dashed curve. A quite distinct phase diagram is obtained for each region of $a \sim d$ with varying u, as illustrated in figure 3.

3.2. Classification of phase diagrams

As has been pointed out by Nara *et al* [8], the lattice-gas Hubbard model can produce quite a variety of types of phase diagram with varying u. In this section, on the basis of the analytic expressions presented in the previous section, we present a general analysis of the relationship between the MNM and the LV transition. In order to see the electronic effects clearly, we make the analysis assuming $j = 0$.

The equilibrium conditions for the first-order phase transition between two phases (1) and (2) with reduced volume $v^{(1)}$ and $v^{(2)}$ respectively at temperature T are obtained as

$$p(v^{(1)}) = p(v^{(2)}) \tag{43}$$
$$\mu_a(v^{(1)}) = \mu_a(v^{(2)}). \tag{44}$$

By using the expressions for p and μ_a given by (38) and (41) in these relations, it can be shown that four types of phase diagram are obtained with varying u. The critical values of volume as a function of u for the first-order phase transitions are shown in figure 2. Note that the curve for $v = v_M = 1/u^2$, shown by the dashed curve in the figure, gives the boundary line for the Mott transition. In the following, the phase on the high-density side of the Mott transition is referred to as metallic, while the one on the low-density side is referred to as non-metallic, although the actual MNM transition may occur at a volume other than v_M due to the effect of disorder combined with the electron correlation. Some further remarks on this point will be given in the following subsection.

Quite distinct types of phase diagram are obtained for each of the four regions $a \sim d$, as shown in this figure, with varying u. Typical examples of the four types of phase diagram on the p–v, p–t, and t–v planes with $u = 0.3, 0.4, 0.5,$ and 0.8 are shown in figure 3. The features of each type of phase diagram are discussed below.

(i) Type a for $0 \leqq u \lesssim 0.374$. In this region of weak electron correlation there occurs a single first-order transition from a metallic liquid (ML) phase to a metallic vapour (MV) phase. Note that, even for the case with no correlation, that is for $u = 0$, this type of first-order transition occurs; the critical values for this case can be obtained easily as

$v_c^{(0)} = 3$, $t_c^{(0)} = 2/(3\pi\sqrt{3}) \approx 0.123$, and $p_c^{(0)} = 2\{3\ln(3/2) - 1\}/(9\pi\sqrt{3}) \approx 0.008\,84$. This ML–MV transition is caused by the feature that, with increasing v, the electronic energy increases due to band narrowing while the entropy of the atomic configurations decreases. The effect of the electron correlation in this range is still weak enough and only causes a slight broad rise of the coexistence curve on the p–v plane in the vicinity of the Mott transition at $v \simeq v_M$, as is demonstrated in figure 3(a) for the case of $u = 0.3$. The corresponding phase diagrams on the p–t and t–v planes are shown in the same figure.

(ii) Type b for $0.374 \lesssim u \lesssim 0.426$. As u increases into this region another first-order transition appears around $v = v_M$ in addition to the ML–MV transition which remains essentially unchanged from the one in the weak-correlation region explained above. Two full curves in region b of figure 2 represent the critical volumes of these first-order transitions. As was pointed out at the end of the previous subsection, $p_e^{(1)}$ below v_M, which is an increasing function of v, grows larger with increasing u but remains small in region b. Therefore the ML–MV transition is not affected much by the electron-correlation effects, and the features of the boundary curves between the coexisting ML and MV phases, as shown in figure 3(b), are almost the same as those for the weak-correlation case, although the critical values of volume, temperature, and pressure become slightly larger. The newly appearing extra phase transition occurs across the Mott transition. As was also mentioned in the previous subsection, $p_e^{(1)}$ as a function of v increases rather abruptly in the vicinity of v_M and then has a peak at $v = (3\pi/8)^2 v_M$. For the values of u in region b the height of this peak grows so high that, even for temperatures near the critical temperature, an extra pair of a maximum and a minimum is produced in isotherms of the total pressure p versus v, as plotted, including the regions of the metastable and unstable states on top of the one associated with the ML–MV transition. Note, however, that, as the second partial derivative of (38) with respect to v is not continuous at $v = v_M$, this newly produced transition is not a usual first-order phase transition. Hence, the critical volume becomes just v_M because $\lim_{v \to v_M - 0} \partial^2 p/\partial v^2 = \infty$. The critical pressure and the critical temperature are obtained from the following equations: $p_c = p(v_M, t_c)$, $(\partial p/\partial v)_{v_M, t_c} = 0$. Some further analyses of the phase diagrams in this region will be given in the following subsection in relation to the peculiar feature of the coexistence curve of fluid Cs.

(iii) Type c for $0.426 \lesssim u \lesssim 1/\sqrt{2}$. When u increases further into this region, the two phase transitions that occurred in region b approach and merge together into a single one between a ML phase and a non-metallic vapour (NMV) phase across the Mott transition, as shown in region c of figure 2. The critical volume of this ML–NMV phase transition is given by $5.6 \lesssim v_c = v_M \leqslant 2$. This type c of the phase diagrams on the p–v, p–t, and t–v planes is demonstrated with $u = 0.5$ in figure 3(c).

(iv) Type d for $u \gtrsim 1/\sqrt{2}$. In this region of strong electron correlation there occurs a single first-order LV phase transition on the non-metallic side of the Mott transition, as shown in the region d of figure 2. The Mott transition, which does not accompany a first-order transition, thus occurs in the liquid phase. The critical volume of the LV transition in this region is analytically obtained as $v_c = 2$ in the standard way, as applied to the usual insulating lattice-gas system. Similarly the coexistence curves illustrated for $u = 0.8$ in figure 3(d) show the same characteristic features as the ones known for the standard lattice-gas theory.

3.3. Application to fluid Cs

Among the four possible types of phase diagram, we particularly notice type b since a strong asymmetry appears in the coexistence curve of this type, which is the peculiar feature observed
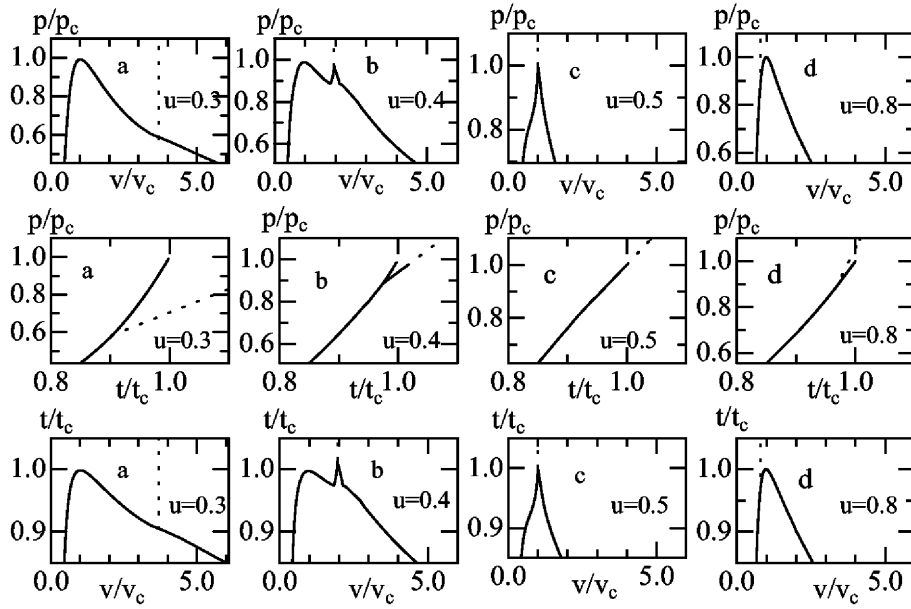
Figure 3. Four types of possible phase diagrams in p–v, p–t and t–v planes illustrated with a typical value of u for each region shown in figure 2. The solid curve shows the coexistence curve. The dashed curve describes the Mott transition accompanying no change of volume.

in experiments. In figure 4 the coexistence curve calculated with $u = 0.425$ ($v_M = 5.536$), shown by the solid curve, is compared with the observed result denoted by the solid circles. The calculated critical values are given by $v_c = 3.2$, $t_c = 0.124$, and $p_c = 0.0105$. The theoretical result resembles quite nicely the observed one except for the fact that the coexistence region around the Mott transition obtained theoretically does not appear in the experimental result. But it is noted that this discrepancy, which manifests itself rather exaggeratedly in figure 4, is quite small if we look at the original p versus v curves, as shown in figure 5, from which the coexistence curves are obtained. The irregularity of the curves around the Mott transition is very slight and looks rather like a plateau extending from the critical region of the ML–MV transition up to around v_M, so, if this is real, it might be very hard to observe the coexistence region around v_M experimentally.

As already mentioned in the preceding sections, the MNM transition as observed from the measurements of the electrical conductivity may occur at a density different from the value for the Mott transition due to the Anderson transition combined with it. As pointed out by Yonezawa and Watabe [7], the Anderson localization in the lattice-gas Hubbard system can be caused by the effects of disorder in both atomic and electronic (spin) configurations. It is well known that the single-site coherent-potential approximation employed in the present theory cannot deal in principle with localization, but by applying the criterion due to Economou and Cohen [15] to the Green function presented in the previous section they estimated that, with increasing v, the Anderson localization of the electronic states near the Fermi level starts to occur at $v = (3 + 2\sqrt{2} + u^2)/(1 + 6u^2 + u^4)$, which lies somewhat below the critical volume of the LV transition for u in region b. This result agrees with the observed results for the electrical conductivity [3].
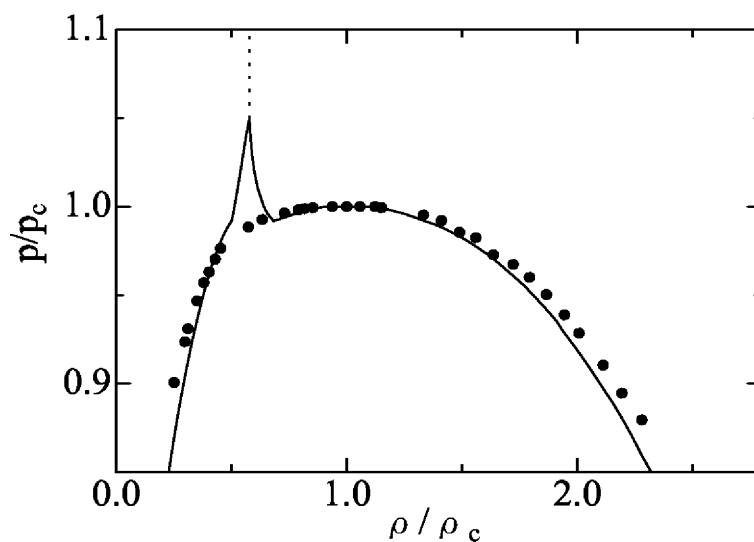
Figure 4. The calculated coexistence curve in the p–ρ plane with $u = 0.425$ denoted by the solid curve is compared with the experimental result for fluid Cs shown by the solid circles (●).
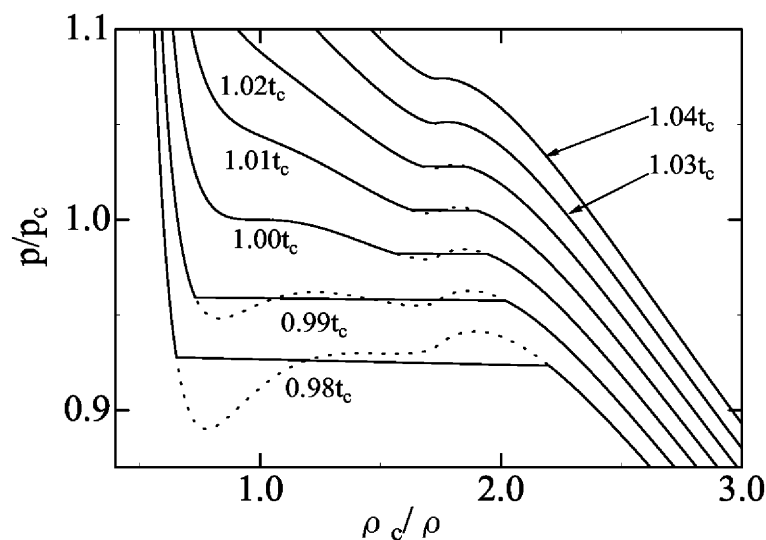

Figure 5. The calculated isothermal p versus v curves for the same system with $u = 0.425$ as shown in figure 4 at various temperatures, $t/t_c = 0.98, 0.99, 1.00, 1.01, 1.02, 1.03$, and 1.04. The states denoted by the dashed curves are either metastable or unstable.

4. Conclusions

For the purposes of investigating the effects of the electron correlation on the thermodynamic properties, especially the observed peculiar behaviour of the coexistence curve, of fluid alkalis in the critical region, we revisited the lattice-gas Hubbard model, investigated extensively in 1970, in the light of the later important developments during these two decades. We consider that, although the present theory is based on more simplified approximations than

those employed in the more recent theories, it is still worth presenting what results are obtained within the well-defined simple and consistent approximations as employed in the present work for developing further advanced theories.

It was pointed out that a variety of types of phase diagram can be obtained by varying the parameter describing the strength of the electron correlation in this model and that, with a proper choice of this parameter in a certain range of intermediate strength, it is possible to obtain a phase diagram which reproduces a quite asymmetric coexistence curve resembling the one observed experimentally. The asymmetry in this theory is caused by the existence of an extra phase transition associated with the Mott transition in addition to the rather normal LV transition taken over from the weak-correlation regime. The extra phase transition is caused by the general change of the dependence on volume of the hopping effects across the Mott transition. This result, though derived for a simplified model with several approximations, suggests the possibility of the peculiar behaviour of fluid alkalis such as Cs and Rb in the critical region being due to the effects of electron correlation.

Among the approximations in this theory, the importance of improving the mean-field approximation for atomic arrangements has been pointed out by Reinald-Falagán *et al* [11,12]. They concluded that it is important to treat the local atomic configuration beyond the mean-field approximation self-consistently with the electronic energy to reproduce the asymmetric feature of the LV coexistence curve. It would be desirable to improve the present theory by including the effects beyond the single-site approximations in both atomic and electronic aspects as well as the effect of finite temperature on the electronic free energy for the more realistic model.

As for the other approximation of assuming the underlying lattice structure in the present model, it is pointed out that there have been papers by Yonezawa *et al* [16] and more recently by Logan [17] in which the Hubbard model is extended to apply to systems with some more realistic liquid-like structures. In these papers the effects of structural disorder combined with electron correlation are investigated for the electronic properties of such systems such as electron localization [16, 17], electric conductivity [17], and magnetic susceptibility [17]. It would also be interesting to extend the present theory to include the effect of such structural disorder.

Acknowledgments

Appendix. The expression for the electronic internal energy in terms of the Green function

We define the one-electron retarded Green function in the site representation as

$$G_{ij}^{\sigma}(t) = -\mathrm{i}\theta(t)\xi_i \langle [a_{i\sigma}(t), a_{j\sigma}^{\dagger}(0)]_+ \rangle^{(\mathrm{e})} \xi_j \tag{A.1}$$

where $\langle [\cdots] \rangle^{(\mathrm{e})}$ is the average over the grand-canonical ensemble for the electronic states under a fixed distribution of atoms, given explicitly as

$$\langle (\cdots) \rangle^{(\mathrm{e})} = \mathrm{Tr}^{(\mathrm{e})} \exp\{-\beta(\hat{H}_\mathrm{e} - \mu_\mathrm{e}\hat{N}_\mathrm{e})\}(\cdots)/\hat{\Xi}^{(\mathrm{e})}[\{\xi_i\}] \tag{A.2}$$

with $\hat{\Xi}^{(e)}[\{\xi_i\}] = \exp(-\beta\hat{\Omega}_e[\{\xi_i\}])$ and $a_{i\sigma}(t)$ $(a_{j\sigma}^\dagger(t))$ the annihilation (creation) operator for an electron with spin σ in the Heisenberg representation, defined as

$$a_{i\sigma}(t) = \exp(i\hbar^{-1}\hat{H}_e t)a_{i\sigma}\exp(-i\hbar^{-1}\hat{H}_e t). \tag{A.3}$$

Other notation is as usual: $\theta(t)$ is the step function, $[A, B]_+$ $(=AB+BA)$ the anti-commutator, etc. The equation of motion for the Green function $G_{ij}^\sigma(t)$ is given by

$$i\hbar\frac{\partial G_{ij}^\sigma(t)}{\partial t} = \hbar\delta(t)\delta_{ij}\xi_i + E_0 G_{ij}^\sigma(t) + \sum_{j'(\neq i)}\xi_i V_{ij'}G_{j'j}^\sigma(t) + U I_{ij}^\sigma(t) \tag{A.4}$$

with

$$I_{ij}^\sigma(t) = -i\theta(t)\xi_i\langle[a_{i\sigma}(t)n_{i-\sigma}(t), a_{j\sigma}^\dagger(0)]_+\rangle^{(e)}\xi_j. \tag{A.5}$$

On Fourier transforming with respect to t as follows:

$$G_{ij}^\sigma(E) = \int_{-\infty}^\infty dt\,\exp(iEt/\hbar)G_{ij}^\sigma(t) \tag{A.6}$$

$$I_{ij}^\sigma(E) = \int_{-\infty}^\infty dt\,\exp(iEt/\hbar)I_{ij}^\sigma(t) \tag{A.7}$$

and averaging over atomic configurations, the diagonal part $(i = j)$ of the above equation becomes

$$(E - E_0)\langle G_{ii}^\sigma(E)\rangle^{(a)} - \sum_{j(\neq i)}V_{ij}\langle G_{ji}^\sigma(E)\rangle^{(a)} - \langle U I_{ii}^\sigma(E)\rangle^{(a)} = \hbar\xi \tag{A.8}$$

where

$$\langle(\cdots)\rangle^{(a)} = \mathrm{Tr}^{(a)}\exp\{-\beta(\hat{H}_{eff} - \mu_a\hat{N}_a)\}(\cdots)/\Xi \tag{A.9}$$

with $\Xi = \exp(-\beta\Omega)$. In the wavenumber (k) representation, we can rewrite the above equations as

$$\frac{1}{N}\sum_k\{(E - E(k))G^\sigma(k, E) - U I^\sigma(k, E)\} = \hbar\xi \tag{A.10}$$

where

$$\langle G_{ij}^\sigma(E)\rangle^{(a)} = \frac{1}{N}\sum_k G^\sigma(k, E)\exp\{ik\cdot(R_i - R_j)\} \tag{A.11}$$

$$\langle I_{ij}^\sigma(E)\rangle^{(a)} = \frac{1}{N}\sum_k I^\sigma(k, E)\exp\{ik\cdot(R_i - R_j)\}. \tag{A.12}$$

Here, R_i is the position vector of the site i. Note that $\langle G_{ij}^\sigma(E)\rangle^{(a)}$ and $\langle I_{ij}^\sigma(E)\rangle^{(a)}$ are lattice-translationally invariant (i.e. they depend only on the difference $R_i - R_j$), so they become diagonal in the k-representation. By introducing the self-energy $\Sigma^\sigma(k, E)$ defined by the equation

$$G^\sigma(k, E) = \frac{\hbar}{E + i\delta - E(k) - \Sigma^\sigma(k, E)} \tag{A.13}$$

we obtain the relation expressing $I^\sigma(k, E)$ in terms of $\Sigma^\sigma(k, E)$ as

$$\frac{1}{N}\sum_k U I^\sigma(k, E) = \frac{1}{N}\sum_k \Sigma^\sigma(k, E)G^\sigma(k, E) + \hbar(1 - \xi). \tag{A.14}$$

Using the relation

$$\xi_i \langle a_{i\sigma}^\dagger a_{j\sigma} \rangle^{(e)} \xi_j = -\frac{1}{\pi\hbar} \int_{-\infty}^{\infty} dx \, f(x) \, \text{Im} \, G_{ij}^\sigma(x) \tag{A.15}$$

$$\xi_i \langle n_{i\sigma} n_{i-\sigma} \rangle^{(e)} = -\frac{1}{\pi\hbar} \int_{-\infty}^{\infty} dx \, f(x) \, \text{Im} \, I_{ii}^\sigma(x) \tag{A.16}$$

where

$$f(E) = \frac{1}{\exp\{\beta(E - \mu_e)\} + 1} \tag{A.17}$$

the electronic internal energy can be expressed as

$$\hat{E}_e[\{\xi_i\}] = \langle \hat{H}_e \rangle^{(e)}$$

$$= E_0 \sum_{i,\sigma} \langle n_{i\sigma} \rangle^{(e)} \xi_i + \sum_{i \neq j, \sigma} V_{ij} \langle a_{i\sigma}^\dagger a_{j\sigma} \rangle^{(e)} \xi_i \xi_j + \frac{U}{2} \sum_{i,\sigma} \langle n_{i\sigma} n_{i-\sigma} \rangle^{(e)} \xi_i$$

$$= -\frac{1}{\pi\hbar} \sum_{i,\sigma} \text{Im} \int_{-\infty}^{\infty} dx \, f(x) \left\{ E_0 G_{ii}^\sigma(x) + \sum_{j(\neq i)} V_{ij} G_{ij}^\sigma(x) + \frac{U}{2} I_{ii}^\sigma(x) \right\}. \tag{A.18}$$

Averaging over atomic configurations and using the relations derived above, we finally obtain

$$E_e = \langle \hat{E}_e[\{\xi_i\}] \rangle^{(a)} = -\frac{1}{\pi\hbar} \sum_{k,\sigma} \text{Im} \int_{-\infty}^{\infty} dx \, f(x) \left\{ x - \frac{1}{2} \Sigma^\sigma(k, x) \right\} G^\sigma(k, x). \tag{A.19}$$

The total number of electrons is similarly given by

$$N_e = -\frac{1}{\pi\hbar} \sum_{k,\sigma} \text{Im} \int_{-\infty}^{\infty} dx \, f(x) G^\sigma(k, x). \tag{A.20}$$

References

[1] Yonezawa F (ed) 1982 Metal–nonmetal transitions in random systems *Prog. Theor. Phys. Suppl.* **72**
[2] Yonezawa F and Ogawa T 1982 *Prog. Theor. Phys. Suppl.* **72** 1
[3] Franz G, Freyland W and Hensel F 1980 *J. Physique Coll.* **41** C8 70
[4] Freyland W 1981 *Solid State Commun.* **10** 1
[5] Franz G, Freyland W, Gläser G, Hensel F and Schneider E 1980 *J. Physique Coll.* **41** C8 194
[6] Winter R, Pilgrim and Hensel F 1991 *J. Physique Coll.* **4** C5 45
[7] Yonezawa F and Watabe M 1973 *Phys. Rev.* B **8** 4540
[8] Nara S, Ogawa T and Matsubara T 1979 *Prog. Theor. Phys.* **61** 736
    Ogawa T, Nara S and Matsubara T 1982 *Prog. Theor. Phys. Suppl.* **72** 140
[9] Jüngst S, Knuth B and Hensel F 1985 *Phys. Rev. Lett.* **555** 2160
[10] Jüngst S 1985 *Doctoral Thesis* Universität Marburg (Marburg/Lahn)
[11] Reinaldo-Falagán M, Tarazona P, Chacón E and Hernandez J P 1997 *J. Phys.: Condens. Matter* **9** 9799
[12] Reinaldo-Falagán M, Tarazona P, Chacón E and Hernandez J P 1999 *Phys. Rev.* E **60** 2626
[13] Goldstein R E, Palola A, Ashcroft N W, Pestak M W Chan M H W, de Bruin J R and Balzarini 1986 *Phys. Rev. Lett.* **58** 41
[14] Kubo R 1962 *J. Phys. Soc. Japan* **17** 1100
[15] Economou E N and Cohen M H 1972 *Phys. Rev.* B **5** 2931
[16] Yonezawa F, Watabe M, Nakamura M and Ishida Y 1974 *Phys. Rev.* B **10** 2322
[17] Logan D E 1991 *J. Chem. Phys.* **94** 628